NAVAL POSTGRADUATE SCHOOL

MONTEREY, CALIFORNIA

THESIS

PERFORMANCE AND COMPLEXITY TRADE STUDY OF CANDIDATE LIQUID AIR GENERATION TECHNIQUES

by

Masis B. Torosyan

June 2021

Thesis Advisor:	Anthony G. Pollman
Co-Advisor:	Alejandro S. Hernandez

THIS PAGE INTENTIONALLY LEFT BLANK

REPORT DOCUMENTATION PAGE				*Form Approved OMB No. 0704-0188*
Public reporting burden for this collection of information is estimated to average 1 hour per response, including the time for reviewing instruction, searching existing data sources, gathering and maintaining the data needed, and completing and reviewing the collection of information. Send comments regarding this burden estimate or any other aspect of this collection of information, including suggestions for reducing this burden, to Washington headquarters Services, Directorate for Information Operations and Reports, 1215 Jefferson Davis Highway, Suite 1204, Arlington, VA 22202-4302, and to the Office of Management and Budget, Paperwork Reduction Project (0704-0188) Washington, DC, 20503.				
1. AGENCY USE ONLY ***(Leave blank)***	**2. REPORT DATE** June 2021	**3. REPORT TYPE AND DATES COVERED** Master's thesis		
4. TITLE AND SUBTITLE PERFORMANCE AND COMPLEXITY TRADE STUDY OF CANDIDATE LIQUID AIR GENERATION TECHNIQUES				**5. FUNDING NUMBERS**
6. AUTHOR(S) Masis B. Torosyan				
7. PERFORMING ORGANIZATION NAME(S) AND ADDRESS(ES) Naval Postgraduate School Monterey, CA 93943-5000				**8. PERFORMING ORGANIZATION REPORT NUMBER**
9. SPONSORING / MONITORING AGENCY NAME(S) AND ADDRESS(ES) N/A				**10. SPONSORING / MONITORING AGENCY REPORT NUMBER**
11. SUPPLEMENTARY NOTES The views expressed in this thesis are those of the author and do not reflect the official policy or position of the Department of Defense or the U.S. Government.				
12a. DISTRIBUTION / AVAILABILITY STATEMENT Approved for public release. Distribution is unlimited.				**12b. DISTRIBUTION CODE** A

13. ABSTRACT (maximum 200 words)

This paper presents the results of an alternatives analysis of gas-liquefaction methods used in liquid air energy storage (LAES) systems that incorporates two novel measures of performance (MOP) into the analysis: system complexity score and system density. The cryogenic methods typically considered for air, and used in this trade study, include Linde-Hampson, Claude, Heylandt, and cascade. With these four options of air liquefaction currently in use for a variety of purposes with ranging scales, there exists no standard selection process for the air-liquefaction method in LAES. This trade study provides fundamental design solutions for given stakeholder requirements, allowing for a pragmatic analysis of integration for future implementation of LAES systems. The intent of these design solutions is for use in the earliest stage of consideration of a LAES implementation, helping stakeholders quickly narrow the focus of their design engineers to a specific liquefaction process. This will reduce the complexity of integration techniques and processes and streamline LAES into the energy-storage industry. The results of this study showed that with evenly weighted MOP, the Heylandt method had the highest final weighted score (0.9), followed by cascade (0.88), Claude (0.86), and Linde-Hampson (0.67). However, the results showed that the cascade method was the most frequent design solution (8/11) from 11 variations of MOP weight distributions.

14. SUBJECT TERMS LAES, Claude, Heylandt, Linde-Hampson, cascade, energy storage, gas liquefaction			**15. NUMBER OF PAGES** 55
			16. PRICE CODE
17. SECURITY CLASSIFICATION OF REPORT Unclassified	**18. SECURITY CLASSIFICATION OF THIS PAGE** Unclassified	**19. SECURITY CLASSIFICATION OF ABSTRACT** Unclassified	**20. LIMITATION OF ABSTRACT** UU

NSN 7540-01-280-5500

Standard Form 298 (Rev. 2-89) Prescribed by ANSI Std. 239-18

THIS PAGE INTENTIONALLY LEFT BLANK

Approved for public release. Distribution is unlimited.

PERFORMANCE AND COMPLEXITY TRADE STUDY OF CANDIDATE LIQUID AIR GENERATION TECHNIQUES

Masis B. Torosyan
Lieutenant, United States Navy
BA, University of Southern California, 2015

Submitted in partial fulfillment of the
requirements for the degree of

MASTER OF SCIENCE IN SYSTEMS ENGINEERING

from the

NAVAL POSTGRADUATE SCHOOL
June 2021

Approved by: Anthony G. Pollman
Advisor

Alejandro S. Hernandez
Co-Advisor

Ronald E. Giachetti
Chair, Department of Systems Engineering

THIS PAGE INTENTIONALLY LEFT BLANK

ABSTRACT

This paper presents the results of an alternatives analysis of gas-liquefaction methods used in liquid air energy storage (LAES) systems that incorporates two novel measures of performance (MOP) into the analysis: system complexity score and system density. The cryogenic methods typically considered for air, and used in this trade study, include Linde-Hampson, Claude, Heylandt, and cascade. With these four options of air liquefaction currently in use for a variety of purposes with ranging scales, there exists no standard selection process for the air-liquefaction method in LAES. This trade study provides fundamental design solutions for given stakeholder requirements, allowing for a pragmatic analysis of integration for future implementation of LAES systems. The intent of these design solutions is for use in the earliest stage of consideration of a LAES implementation, helping stakeholders quickly narrow the focus of their design engineers to a specific liquefaction process. This will reduce the complexity of integration techniques and processes and streamline LAES into the energy-storage industry. The results of this study showed that with evenly weighted MOP, the Heylandt method had the highest final weighted score (0.9), followed by cascade (0.88), Claude (0.86), and Linde-Hampson (0.67). However, the results showed that the cascade method was the most frequent design solution (8/11) from 11 variations of MOP weight distributions.

THIS PAGE INTENTIONALLY LEFT BLANK

TABLE OF CONTENTS

THIS PAGE INTENTIONALLY LEFT BLANK

LIST OF FIGURES

THIS PAGE INTENTIONALLY LEFT BLANK

LIST OF TABLES

THIS PAGE INTENTIONALLY LEFT BLANK

LIST OF ACRONYMS AND ABBREVIATIONS

CA	Cascade (method)
CL	Claude (method)
HT	Heylandt (method)
JT	Joule-Thompson
LH	Linde-Hampson (method)
LAES	liquid air energy storage
MOP	measure of performance
PFOM	performance figure of merit
SCS	system complexity score

THIS PAGE INTENTIONALLY LEFT BLANK

EXECUTIVE SUMMARY

The Achilles' heel of renewable energy is its energy storage infrastructure. The most common energy storage solutions in use are compressed air energy storage (CAES), pumped hydroelectric storage (PHS), or large lithium-ion batteries; but in comparison to these alternatives, liquid air energy storage (LAES) is a lower-cost solution for a higher-power, longer-duration, and more scalable system (Highview Power 2020), with its greatest advantage being its significantly higher energy density.

LAES, however, has several variants that use different liquefaction methods, each with specific trade-offs. These variations ultimately show that there is no single generic method for the liquefaction of air in the charging stage of LAES. The gas-liquefaction methods typically considered for air include Linde-Hampson, Claude, Heylandt, and cascade (Barron 1985, ix–x). While LAES has shown a promising future in energy storage, it requires a concise and consolidated source that describes the benefits and take-aways from each liquid air liquefaction method based on varying stakeholder requirements necessary for implementation. Using the most appropriate LAES system for a set of given requirements will assist in the reduction of the complexity of integration techniques and processes and streamline LAES into the energy-storage industry.

The following methodology introduces a novel method of comparing and contrasting gas-liquefaction methods used in LAES. This trade study targets two measures of performance (MOP): a system complexity score (SCS) and a performance figure of merit (PFOM). The first MOP of the liquefaction methods is the performance figure of merit (PFOM) and is defined as "the theoretical minimum work requirement divided by the actual work requirement for the system" (Barron 1985). This produces a value between 0 and 1, representing how closely the actual system approaches the ideal system performance (Barron 1985).

The second MOP used is the system complexity score (SCS). This thesis proposes two novel measures to compute the system complexity: system density and the system complexity score. This definition allows for more specific and relevant analysis of gas-liquefaction methods. The SCS is derived from the system density and the number of unique node functions. The system density is defined as the ratio of the total number of connection points and total number of nodes. The number of unique functional requirements is a function of the nodes of the system. For example, a system that has three heat exchangers, three compressors, and a reservoir has seven nodes with three node functions. `

The system complexity score (SCS) scales linearly as a function of system density and the number of unique node functions, resulting in a higher SCS for a higher complexity system. SCS is defined as the system density multiplied by the number of unique node functions. This relationship allows for the system with redundant nodes (with respect to functionality) to produce a smaller SCS than a system with the same number of nodes, all with unique functional requirements. This thesis proposes the two previously discussed MOPs to guide the design solution analysis. The PFOM and SCS uses an additive weighting and scaling method that scales raw data of the alternatives to attain comparable units of measurement for analysis. Rather than assuming a generic weight for each MOP and providing a singular solution, it utilizes a decision matrix that considers multiple combinations of assigned weights, calculating each final weighted score to display the appropriate design solution (i.e., liquefaction method) for each selection.

Theoretical values for thermodynamic cycles, particularly ones that assume ideal processes, can often be far from the true or *observed* experimentally tested values. Understanding this, there is a second design matrix that utilizes only the observed PFOM values from experiments by M. Ruhemann and W. Ball as the *R* when calculating the final weighted scores and design solutions (Ruhemann 1949; Ball 1954).

Figure 1 and Figure 2 are the full design solutions for 11 differently weighted MOP variations. Figure 1 utilizes the theoretically derived values, and Figure 2 utilizes the observed values from Ruhemann's and Ball's experiments. Each cell applies the same additive weighting and scaling method, outputting the highest rated method for that set of inputs: Linde-Hampson (LH), Claude (CL), Heylandt (HT), and cascade (CA).

Performance FOM Weight (columns); System Complexity Score Weight (rows)

	0	0.1	0.2	0.3	0.4	0.5	0.6	0.7	0.8	0.9	1
1	**LH**	LH	LH	LH	CL	CL	CL	CL	CL	CL	CL
0.9	LH	**LH**	LH	CL	CL	CL	CL	CL	CL	CL	CL
0.8	LH	LH	**LH**	CL	CL	CL	CL	CL	CL	CL	CL
0.7	LH	LH	LH	**CL**	CL	CL	CL	CL	CL	CL	CL
0.6	LH	LH	CL	CL	**CL**	CL	CL	CL	CL	CL	CL
0.5	LH	LH	CL	CL	CL	**CL**	CL	CL	CL	CL	CL
0.4	LH	LH	CL	CL	CL	CL	**CL**	CL	CL	CL	CL
0.3	LH	CL	CL	CL	CL	CL	CL	**CL**	CL	CL	CL
0.2	LH	CL	CL	CL	CL	CL	CL	CL	**CL**	CL	CL
0.1	LH	CL	CL	CL	CL	CL	CL	CL	CL	**CL**	CL
0	LH	CL	CL	CL	CL	CL	CL	CL	CL	CL	**CL**

Figure 1. Design Solution Matrix Given Theoretical Values

Performance FOM Weight (columns); System Complexity Score Weight (rows)

HT	0	0.1	0.2	0.3	0.4	0.5	0.6	0.7	0.8	0.9	1
1	**LH**	LH	LH	LH	HT	HT	HT	HT	HT	HT	HT
0.9	LH	**LH**	LH	LH	HT	HT	HT	HT	HT	HT	HT
0.8	LH	LH	**LH**	LH	HT	HT	HT	HT	HT	HT	HT
0.7	LH	LH	LH	**HT**	HT	HT	HT	HT	HT	HT	HT
0.6	LH	LH	LH	HT	**HT**	HT	HT	HT	HT	HT	HT
0.5	LH	LH	HT	HT	HT	**HT**	HT	HT	HT	HT	HT
0.4	LH	LH	HT	HT	HT	HT	**HT**	HT	HT	HT	HT
0.3	LH	LH	HT	HT	HT	HT	HT	**HT**	CA	CA	CA
0.2	LH	HT	HT	HT	HT	HT	CA	CA	**CA**	CA	CA
0.1	LH	HT	HT	CA	CA	CA	CA	CA	CA	**CA**	CA
0	LH	CA	CA	CA	CA	CA	CA	CA	CA	CA	**CA**

Figure 2. Design Solution Matrix Given Observed Values

The Claude and Heylandt methods for air liquefaction show both the highest values for liquid yield and the highest levels of exergetic efficiency. The Linde-Hampson is by far the least effective alternative for air liquefaction, but its simplicity is unmatched when compared to the alternatives. The cascade method, although not under comparison for theoretical performance, does retain the highest observed PFOM but requires serious planning considerations due it its high level of system complexity.

This novel method for an analysis of alternatives of gas-liquefaction methods used in LAES systems was designed around providing stakeholders with the necessary information to select the appropriate liquefaction method for their set of given requirements. The easy-to-use design solution matrices provide the simplification of LAES gas-liquefaction methods that is necessary for implementation.

Reference List

Ball, William. 1954. “Freon Cascade Refrigerator for Liquid Air Plant Precooler.” *Refrigerating Engineering* 62: 54–46.

Barron, Randall F. 1985. *Cryogenic Systems*. Second Edition. Oxford University Press.

Highview Power. 2020. “Liquid Air Energy Storage: Clean, Cost-Efficient, Flexible and Reliable.” Highview Power. 2020. https://highviewpower.com/wp-content/uploads/2020/09/Highview-Brochure-Final-2020-1.pdf.

Ruhemann, M. 1949. *The Separation of Gases*. Fair Lawn, NJ: Oxford University Press

ACKNOWLEDGMENTS

I would like to thank Dr. Pollman for his continued support and encouragement in writing this thesis. The advice and assistance shared with me carried more than engineering principles and technical writing guidance, and I am grateful to bring these lessons forward with me into my career.

I would like to thank my mom. She was my biggest fan and most encouraging supporter. This was most evidently seen when she would ask to read my technical papers on sensors and gas liquefaction knowing she did not have a single math-inclined cell in her body. Although today she stands in glory with her Savior, the wisdom and guidance that was gifted to me will be cherished, and I will strive to gift as much God-given joy to my children as has been gifted me.

Lastly, I would like to thank my wife. Completing a master's degree and writing a thesis while in quarantine with two children under 3 is no small feat, which is why this work would not have been possible without the support of Araz, my Pretty Lady. Her selflessness and love were shown not only in how she took care of, kept occupied, or controlled the kids, but how she *loved* on them through it all. This was even more pronounced as we lost Mom this past Christmas. I know the pain of losing her was nearly as much to you as it was to me, and yet you were steadfast. Steadfast for our children and for me. I know the road we have ahead is not the easiest, but I stand confident in the grace of our Savior, and in the wife he has given me.

"She is clothed in strength and dignity; she can laugh at the days to come."

Proverbs 31:25

THIS PAGE INTENTIONALLY LEFT BLANK

I. INTRODUCTION AND BACKGROUND

In the name of social, environmental, and economic progress, the energy market is transitioning to renewable power (Highview Power 2020). In 2015, 195 nations came together in Paris for the United Nations Framework Convention on Climate Change's (UNFCCC) 21st Conference of Parties (COP21) (Denchak 2018). After two weeks of deliberations, they arrived at a consensus now called the Paris Agreement in which they decided to strive towards carbon neutral emissions by 2050, among other goals (Denchak 2018). Although the United States formally withdrew from the Paris Agreement in November of 2019 to late January of 2021, the State of New York has set a plan to be fully carbon-neutral by 2040 (New York Department of Environmental Conservation 2019); Washington State, Maine, Hawaii, New Mexico and California by 2045 (Washington State Department of Commerce 2019; Mills 2019; Office of the Governor of Hawaii 2018; Office of the Governor of New Mexico 2019; California Energy Commission 2018); New Jersey by 2050 (State of New Jersey 2019); and many other states are on their way to enacting similar legislation.

While these are all fairly recent policy enactments, renewable energy's share in global electricity generation increased from 18 to 30 percent from 2007 to 2020 and accounts for nearly 29 percent of electricity in the European Union (EU) as of 2018, a 12 percent increase for the EU since 2008 (IEA 2020; Eurostat 2020). Renewable energy that is clean, but inherently intermittent, has grown so rapidly worldwide over the last couple of decades that it became on par with natural gas as of 2013 (Jaraite, Karimu, and Kazukauskas 2017). This massive growth in renewable energy systems via governmental policies has put a spotlight on the numerous technological shortfalls it faces when integrating into the developed world.

Since conception, the primary concern of renewable energy was the ability to produce consistent and sufficient power as required. Renewable energy systems such as wind, solar, or hydro power generate electricity regardless of demand. The most efficient wind turbines in the world still produce no electricity when there is no wind. However, with the immense growth of the industry, serious advances in innovation have allowed these systems to often be more than sufficient and regularly surpass the average energy required. The question of sufficiency has seemed to have swung the other direction towards overproduction. Currently, renewable energy generation's problem is efficiency. Not efficiency in power generation, but long-term efficiency: efficiency that measures overproduction that is wasted away in resistor banks, power that the system wished it had on cloudy, windless days as the grid is being strained by peak power usage. This problem, however, may be much easier to solve.

Although governments and corporations cannot control the environment, if electrical grids were able to leverage the overproduction of energy towards periods of low production and peak energy usage, they would achieve ideal efficiency. William Pickard discusses this as what he calls the "Achilles' heel of renewable energy" in a paper focusing on whether the "needed [energy] storage infrastructure [can] be constructed before the fossil fuel runs out" (Pickard 2014, 1094). According to New Jersey's Energy Master Plan Policy Vision to 2050,

> Energy storage is a way of capturing excess energy when the sun is shining and the wind is blowing, and providing that energy back to the grid when renewable generation ceases. Energy storage also provides ancillary services, such as regulating grid frequency. Finally, storage systems can shave peak load by providing energy back to the grid during peak demand. Integrating storage into the energy system and further advancing the technology is critical to providing clean, reliable, and resilient energy going forward. (State of New Jersey 2019, 100)

The most common answers to this energy storage problem have been compressed air energy storage (CAES), pumped hydroelectric storage (PHS), or large lithium-ion batteries. Table 1 shows a more detailed comparison of the energy storage between compressed and liquid air, specifically displaying that the density of liquid air at 1 bar is nearly 9 times greater than the density of compressed air at 100 bar (Sixian et al. 2015).

Table 1. Comparison of CAES and Liquid Fluid Energy Storage. Source: Sixian et al. (2015, 731).

	Density kg/m3	Energy Density kJ/Litre
Compressed air (100 bar, 150 C)	115.4	34.8
Compressed air (200 bar, 150 C)	221.84	70.07
Liquid air (1 bar, saturated)	983.56	296.6

Overall, these alternative methods (CAES, PHS, batteries) have glaring limitations in that they are either too expensive, geographically limited, or serviceable to only specific ranges of energy needs (e.g., 1–10MW, 100–1000MW) (Nelmes 2015). The rush towards carbon neutral policies has, however, caused the energy storage industry to see “significant cost improvements, increased manufacturing capacity, large investments and ongoing R&D during 2019, with many of these activities focused on short-duration storage applications and battery technologies” (REN21 2020, 24). With the current policy rush towards carbon neutral economies, R&D of short-duration storage applications only solve a small portion of the overwhelming problem. New Jersey’s Energy Master Plan discusses how battery energy storage does “provide more flexible, modular, and mobile options,” but “they are simply not currently cost effective for most storage applications” (State of New Jersey 2019, 57). Even with the quickly falling prices of the predominant Lithium-ion battery storage systems, they simply are not likely to be cost-competitive through 2030 (State of New Jersey 2019, 57).

Liquid air energy storage (LAES) is a type of cryogenic energy storage (CES) that is relatively unheard of and a severely untapped system in the energy community. In comparison to the currently available alternatives, LAES is a low-cost solution for a high-power, long-duration, and scalable system that can be built anywhere (Highview Power 2020). LAES’s greatest advantage is the high energy density when compared to batteries, chemical energy storage, pumped hydro, or CAES (Högberg and Tholander 2018).

LAES works in a three-stage process: charging, storage, and recovery. Charging the system consists of drawing air from the surrounding environment and cooling it through varying series and combinations of compressors and heat exchangers until it reaches an expansion valve that utilizes the Joule-Thomson (JT) effect (JT valve), causing the air to drop to a temperature low enough to liquify. Typically, 1 liter of liquid air is produced from 700 liters of ambient air (Energy Storage Association 2020). This liquid air is then stored in insulated tanks at low pressure until power is required. In the last stage, power recovery, the liquid air is pumped out, evaporated and superheated to ambient temperature, causing rapid re-gasification and a 700-fold expansion in volume, “which is then used to drive a turbine” and generate electricity without combustion (Energy Storage Association 2020; Highview Power 2020).

As alluded to earlier, there is no single method for the liquefaction of air in the charging stage of LAES. There are many different types of gas-liquefaction systems available and currently in use for a variety of purposes, each with their own variants, and each with specific trade-offs. The gas-liquefaction methods that are typically considered for air include Linde-Hampson, Claude, Heylandt, and cascade (Barron 1985, ix–x).

A. PROBLEM STATEMENT

While LAES has shown a promising future in energy storage, it requires a concise and consolidated source that describes the benefits and take-aways from each liquid air liquefaction method based on varying stakeholder requirements necessary for implementation. Using the most appropriate LAES system for a set of given requirements will assist in the reduction of the complexity of integration techniques and processes and streamline LAES into the energy-storage industry.

B. RESEARCH OBJECTIVE

This thesis executes a trade-off analysis of four different gas-liquefaction methods (Linde-Hampson, Claude, Heylandt and cascade) used within LAES systems regarding two measures of performance (MOP): system complexity and a performance figure of merit (PFOM). This trade study provides fundamental design solutions for given stakeholder requirements, allowing for a pragmatic analysis of integration for future implementation of LAES systems.

II. METHODOLOGY

The following methodology introduces a novel method of comparing and contrasting gas-liquefaction methods used in LAES. This trade study targets two measures of performance (MOP): a system complexity score (SCS) and a performance figure of merit (PFOM). These MOP are calculated using the fundamental schematics and concepts of each method allowing utility for a broader range of stakeholders facing wide ranging requirements and limitations. The first section of this chapter discusses the overall architecture of the implemented methodology with respect to V-model. Sections B and C of this chapter will discuss the derivation and merits of each MOP used in analysis, whilst the last section will describe how these MOP are used together to give final and overall design solutions.

A. V-MODEL APPROACH

The follow-on analysis to the trade study utilizes a variant of the generic SE V-model. The V-model approach was developed by systems engineers to graphically display the design-build-test process for large and complex engineering projects (Warner 2019). Within the SE community, many variations of this model exist, although all models follow the same general approach.

The left side of the V-model shows in Figure 1 illustrates the development and refinement of requirements, starting at the system level and decomposing down to the item level design requirements. These requirements are the basis for the derived design solution that is passed over to the domain engineers who take the lead for the implementation and integration of the system (Graessler, Hentze, and Bruckmann 2018). The right side of the V-model, as shown, represents the integration of parts and their verification and validation (V&V). Although V&V is on the right side of the V-model, it plays a part all throughout the development process. The blue arrows pointed in both directions in the middle of Figure 1 illustrate both the prospective and retrospective processes of V&V.

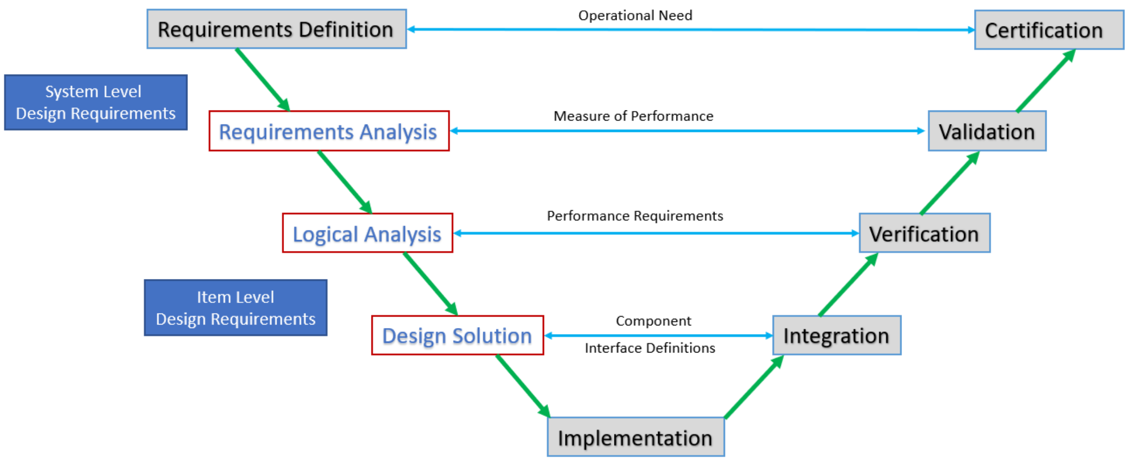

Figure 1. SE V-Model

The three blocks highlighted in red on the left-side of Figure 1 display the portion of the V-model that this thesis follows from the perspective of each of the four methods: Linde-Hampson, Claude, Heylandt, and cascade. The MOP developed by the requirements analysis follows the performance and complexity metrics from the trade study of LAES methods. However, specific to each stakeholder's varying requirements, each of these factors weigh differently. For example, when implementing an LAES system for a city, performance requirements would be emphasized more than complexity concerns given the resources are at the city's disposal; the opposite would be true for a small factory or university campus where a *working* system is the only significant requirement. The analysis of alternatives in this thesis, defined as logical analysis in Figure 1, takes the system-level MOPs and scales them against one another to help provide the appropriate design solution.

B. THEORETICAL PERFORMANCE FIGURE OF MERIT (PFOM)

The first MOP of the liquefaction methods is the theoretical performance. Three values determine the efficiency, or performance, of a liquefaction system: work requirement for gas compressed ($-\dot{w}/\dot{m}$), work required for gas liquefied ($-\dot{w}/\dot{m}_f$), and the fraction of the total flow of gas that had been liquefied ($y = \dot{m}_f/\dot{m}$) (Barron 1985). These performance indicators are related by the following equation.

$$\left(-\frac{\dot{w}}{\dot{m}}\right)=\left(-\frac{\dot{w}}{\dot{m}_f}\right)y \tag{1}$$

Since the result from this equation will differ greatly for various gases, a figure of merit (FOM) allows for comparisons of the same system when using different working fluids (Barron 1985). Although this thesis focuses on air as the working fluid, using the standard FOM will allow for comparative analysis in future works.

The FOM of a gas-liquefaction system, shown in Equation 2, is defined as "the theoretical minimum work requirement divided by the actual work requirement for the system" (Barron 1985).

$$FOM=\frac{\dot{w}_i}{\dot{w}}=\frac{-\dot{w}_i\,/\,\dot{m}_f}{-\dot{w}\,/\,\dot{m}_f} \tag{2}$$

This will produce a value between 0 and 1, representing how closely the actual system approaches the ideal system performance (Barron 1985).

Randall Barron in his book *Cryogenic Systems* (1985) outlines five performance parameters that would apply to a real gas-liquefaction system:

1. Compressor and expander adiabatic efficiencies
2. Compressor and expander mechanical efficiencies
3. Heat-exchanger effectiveness
4. Pressure drops throughout the system
5. Heat transfer from ambient surroundings

Within this thesis's evaluation of performance, all the component efficiencies and effectiveness shall be assumed as ideal. For example, heat exchangers are assumed to be 100 adiabatic and have no irreversible pressure losses (Barron 1985). All liquefaction systems' performance calculations assume an initial air temperature of 300 K and a pressure of 101.3 kPa (1 atm).

To have a standard means of comparison, the PFOM values of each method will be set against the thermodynamically ideal system (ideal reversable system).

C. SYSTEM COMPLEXITY

The varying definitions of the term *complexity* can be broken down into three categories (Seth, n.d.):

1. How hard is it to create?

2. How hard is it to describe?

3. What is the degree of organization?

The difficulty to create is typically computed and measured in time, power, or money. Examples include thermodynamic depth, time computational complexity, and crypticity (Seth, n.d.). The difficulty to describe is often computed and measured in bits. Examples include the Kolmogorov algorithmic complexity, Renyi Entropy, and Fisher information (Watanabe 1992). The last complexity definition of organization can be broken up into two sub-categories: "[The] difficulty of describing organizational structure, whether corporate, chemical, cellular, etc.," and the "amount of information shared between the parts of a system as the result of this organizational structure" (Seth, n.d.). Examples include Stochastic complexity, hierarchical complexity, and channel capacity. As shown, complexity's definitions depend on context and field of study, albeit most of them are defined within computational sciences.

This thesis proposes two novel measures to compute the system complexity: system density and the system complexity score. This definition allows for more specific and relevant analysis of gas-liquefaction methods. The second MOP used in this trade-study, system complexity, is derived from the system density and the number of unique node functions. The system density is defined as the ratio of the total number of connection points and total number of nodes.

$$System\,Density = \left[\frac{Connections\,Points}{Nodes}\right] \tag{3}$$

The number of unique functional requirements is a function of the nodes of the system. For example, a system that has three heat exchangers, three compressors, and a reservoir has seven nodes with three node functions. `

The system complexity score (SCS) scales linearly as a function of system density and the number of unique node functions, allowing for a higher SCS for a higher complexity system. SCS is defined in Equation 4 as the system density multiplied by the number of unique node functions.

$$SCS = System\,Density \times Unique\,Node\,Functions \tag{4}$$

This relationship allows for the system with redundant nodes (with respect to functionality) to produce a smaller SCS than a system with the same number of nodes, all with unique functional requirements. These complexity calculations do not consider the entire LAES system, rather just the liquid air generation side.

D. DESIGN SOLUTION

This thesis proposes the two previously discussed MOPs to guide the design solution analysis. The PFOM and SCS uses an additive weighting and scaling method that is shown in Table 2. This approach scales raw data of the alternatives to attain comparable units of measurement for analysis. After both the MOP and stakeholder assigned weights of importance (W) are assigned, you take every raw MOP value (R) and divide it by the best (not necessarily highest) *R* of the entire lot of alternatives, giving a scaled MOP value (S). Now that each *R* is normalized, it is multiplied by the assigned weight of the MOP, giving a weighted MOP score (WS). Once this process is completed for each MOP, the *WS* of each MOP that were once in incompatible units, are added together to give a final weighted score, where higher scores are better.

Table 2. Additive Weighting and Scaling

	MOP	MOP(A)	MOP(B)	Total
	Weight	W(A)	W(B)	W(1)+W(2)
Alternative A	Raw Value (R)	R(1)	R(2)	
	Scaled Value (S)	S(1) [R(1) / best R]	S(2) [R(2) / (best R)]	
	Wtd. Score (WS)	WS(1) [W(A) x S(1)]	WS(2) [W(B) x S(2)]	Final Wtd. Score [WS(1) +WS(2)]

For this thesis, rather than assuming a generic weight for each MOP and providing a singular solution, it utilizes a decision matrix that considers a multiple combinations of assigned weights, calculating each final weighted score to display the appropriate design solution (i.e., liquefaction method) for each selection.

Theoretical values for thermodynamic cycles, particularly ones that assume ideal processes, can often be far from the true or *observed* experimentally tested values. Understanding this, there is a second design matrix that utilizes only the observed PFOM values from experiments by M. Ruhemann and W. Ball as the *R* when calculating the final weighted scores and design solutions (Ruhemann 1949; Ball 1954).

III. ANALYSIS OF ALTERNATIVES

The analysis of alternatives decomposes the four gas-liquefaction methods into their most basic schematics. These schematics are the basis for the prescribed SCS of each method as well as the derived First Law steady flow equations used in calculating each PFOM.

A. LINDE-HAMPSON METHOD

The Linde-Hampson method for gas-liquefaction is known for its simplicity, and was the second system to liquify gas (Howe 2018). The specific version considered in this thesis analyzes the Simple Linde-Hampson method, as opposed to the alternatives; the Precooled Linde-Hampson and Linde dual-pressure methods (Barron 1985).

The process of the Simple Linde-Hampson method is shown in Figure 2. Ambient gas ($\dot{m}$) is isothermally and reversibly compressed from state 1 to 2. The compressed gas is then cooled in an isobaric heat exchanger (regenerator) to state 3 and expanded through a Joule Thompson (JT) valve to state 4, the rapid expansion of the gas to ambient pressure has now caused a portion of the gas to liquefy ($\dot{m}_f$) and drop into the liquid reservoir, with the remaining gas used to pre-cool the compressor outlet completing the process from state 5 to 6. Note that at steady-state conditions the makeup gas ($\dot{m}_f$) entering the process is equal to the amount of liquid gas produced (Howe 2018).

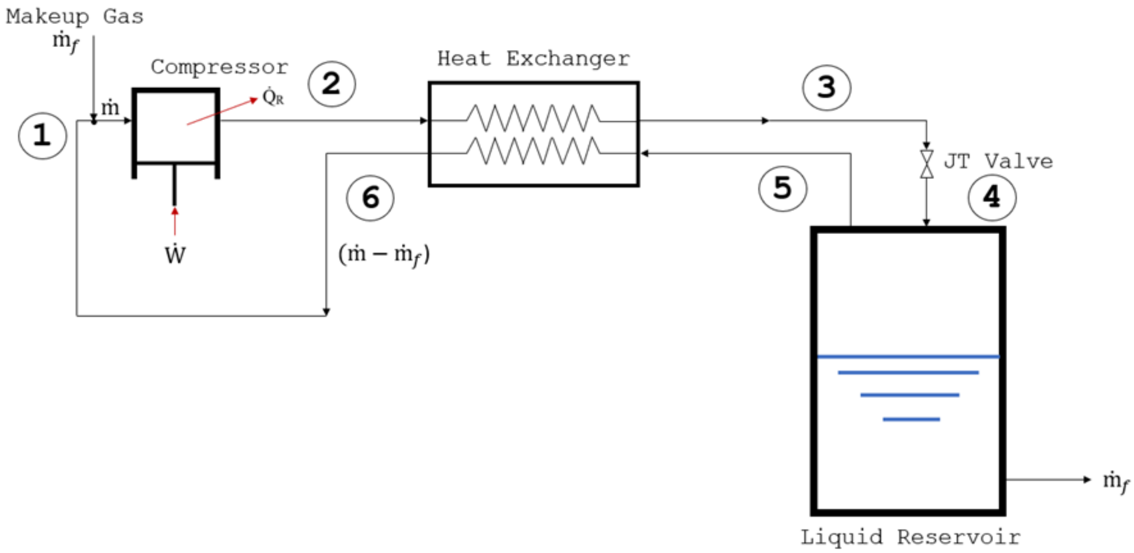

Figure 2. Linde-Hampson Method. Adapted from Barron (1985).

Three functional nodes of this liquefaction system—the heat exchanger, JT valve, and reservoir—can be combined using the First Law for a steady flow shown as Equation 5.

$$0 = \left(\dot{m} - \dot{m}_f\right) h_1 + \dot{m}_f h_f - \dot{m} h_2 \tag{5}$$

Solving this equation for the fraction of liquified gas (y) gives

$$y = \frac{\dot{m}_f}{\dot{m}} = \frac{h_1 - h_2}{h_1 - h_f} \ . \tag{6}$$

Equation 6 written in terms of the compressional work requirement gives (Barron 1985)

$$\dot{Q}_R - \dot{W} = \dot{m}\left(h_2 - h_1\right). \tag{7}$$

From the Second Law of Thermodynamics, a reversible and isothermal process gives Equation 8, where s is the entropy of the working fluid (Barron 1985).

$$\dot{Q}_R = \dot{m} T_1 \left(s_2 - s_1\right) = -\dot{m} T_1 \left(s_1 - s_f\right) \tag{8}$$

Substituting $\dot{Q}_R$ from Equation 8 to Equation 7 gives the work requirement for an ideal system (Barron 1985).

$$-\frac{\dot{W}_i}{\dot{m}_f} = T_1\left(s_1 - s_f\right) - \left(h_1 - h_f\right) \tag{9}$$

This work requirement for a system can then be substituted into Equation 7, giving the work requirement per unit mass liquefied, shown as Equation 10 (Barron 1985).

$$-\frac{\dot{W}}{\dot{m}_f} = -\frac{\dot{W}}{\dot{m}y} = \left(\frac{h_1 - h_f}{h_1 - h_2}\right)\left(T_1\left(s_1 - s_2\right) - \left(h_1 - h_2\right)\right) \tag{10}$$

As Barron points out in *Cryogenic Systems*, Equation 6 shows that the amount of liquefied gas depends on two states: the pressure and temperature of the ambient conditions which determine h_1 and h_f, and secondly the pressure following the isothermal compression defining h_2. Therefore, since stakeholders cannot necessarily change the ambient conditions of the air, the performance of the system will only be varied by adjusting the pressure p_2 (state 2 on Figure 2) (Barron 1985). At 300 K, the optimum performance for maximum liquid yield (y) is roughly 40 MPa, however, since most Linde-Hampson systems commonly use 20MPa (Barron 1985). For the purposes of these calculations, this thesis assumes 20.3MPa (200atm).

Randall Barron in *Cryogenic Systems* utilized the Temperature-Enthalpy (T-s) diagram in Appendix A and Equation 9 to find create Table 3, giving the ideal-work of liquefaction for different gases.

Table 3. Ideal-work Requirements for Gas Liquefaction. Adapted from Barron (1985, 63).

Gas	Normal Boiling Point K	Normal Boiling Point R	Ideal Work of Liquefaction $-\dot{W}_i/\dot{m}_f$ kJ/kg	Ideal Work of Liquefaction $-\dot{W}_i/\dot{m}_f$ Btu/lb(m)
Air	78.8	142	738.9	317.7
Argon	87.28	157.1	478.6	205.7
Carbon monoxide	81.6	146.9	768.6	330.4
Hydrogen	20.27	36.5	12,019	5,167
Neon	27.09	48.8	1,335	574
Nitrogen	77.36	139.2	768.1	330.2
Oxygen	90.18	162.3	635.6	273.3

From the T-s diagram in the appendix , we obtain the following properties of air, where *h* is enthalpy and *s* is entropy:

$h_1 = 6.5\ J/g$ at 101.3 kPa (1atm) and 300 K
$h_2 = -2\ J/g$ at 20.3 MPa (200atm) and 300 K
$h_f = -96\ J/g$ at 101.3 kPa (1atm) and saturated liquid
$s_1 = 0.0837\ J/g-K$ at 101.3 kPa (1atm) and 300 K
$s_2 = -1.548\ J/g-K$ at 20.3 MPa (200atm) and 300 K
$s_f = -3.808\ J/g-K$ at 101.3 kPa (1atm) and saturated liquid.

Utilizing Equation 6 to find the liquid yield gives

$$y = \frac{h_1 - h_2}{h_1 - h_f} = 0.0802. \tag{11}$$

The work requirement per unit mass compressed from Equation 9 gives

$$-\frac{\dot{W}}{\dot{m}} = T_1\left(s_1 - s_2\right) - \left(h_1 - h_2\right) = 481.3\frac{J}{g}. \tag{12}$$

And the work per unit mass liquefied from Equation 10 gives

$$-\frac{\dot{W}}{\dot{m}_f} = -\frac{\dot{W}}{\dot{m}y} = 5,800.6\frac{J}{g}. \tag{13}$$

Since the ideal work for the liquefaction of air, from Barron, is 738.9 J/g it follows that the Performance FOM of the Linde-Hampson method of gas liquefaction (from Equation 2) is

$$FOM = \frac{\dot{W}_i / \dot{m}}{\dot{W} / \dot{m}_f} = 0.127. \tag{14}$$

As seen in Figure 2, the method specified has 11 connection points, three nodes, and three unique node functions. Using Equations 3 and 4, it gives a system density score of 3.67 and an overall SCS of 11.

B. CLAUDE METHOD

The schematic of the Claude method is shown in Figure 3. From state 1 to state 2, the ambient gas is isothermally and reversibly compressed to values around 4.05 MPa (50 atm) (Barron 1985). The key difference between the Claude and Linde-Hampson methods is the utilization of the expander. Just prior to point 3, roughly 75 percent of the working liquid is redirected to the expander before joining the main line again to supplement the return flow of the cold side of the heat exchanger (points 6 and 7). In addition to increasing the efficiency of the first two heat exchangers, most Claude systems utilize the expander to assist in compression of the working fluid (Barron 1985). The calculations of specified system's performance assume a flowrate ratio of 70 percent to the expander, with a 270 K inlet temperature at a pressure of 4.05 MPa, and they assume that the expander aids in compression.

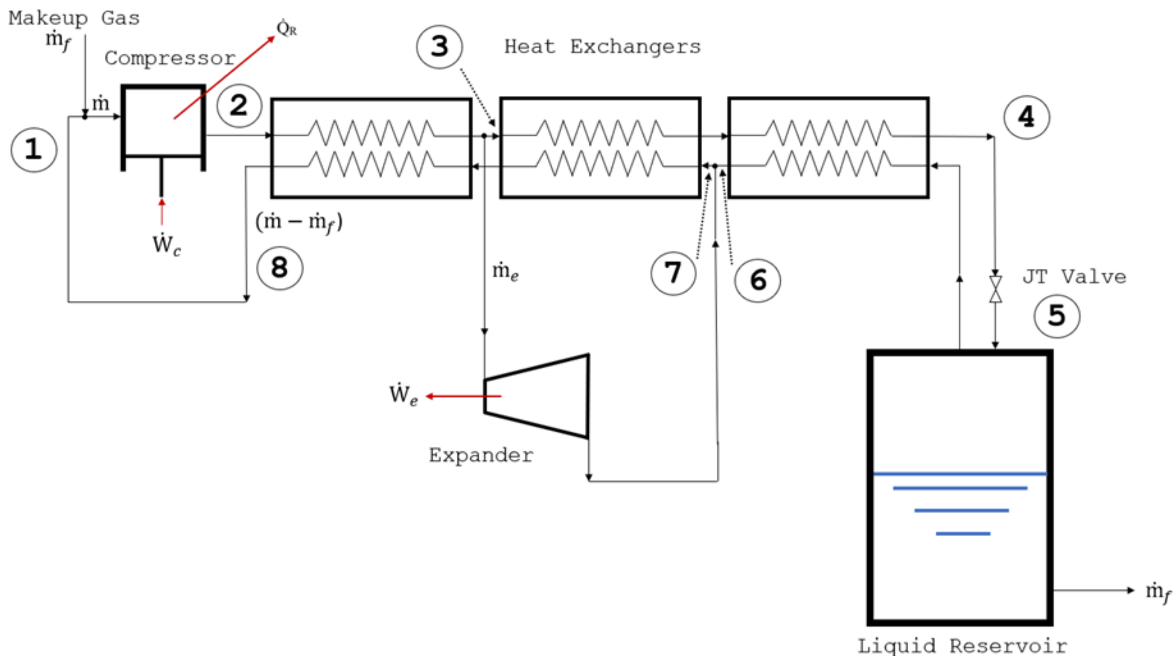

Figure 3. Claude Liquefaction System. Adapted from Barron (1985).

Using the First Law for steady flow for the three function nodes of the Claude liquefaction system gives, (Barron 1985)

$$0 = \left(\dot{m} - \dot{m}_f\right) h_1 + \dot{m}_f h_f + \dot{m}_e h_e - \dot{m} h_2 - \dot{m}_e h_3 \ , \tag{15}$$

where the flow through the expander as a fraction of the total flow (x) is defined as

$$x = \frac{\dot{m}_e}{\dot{m}} . \tag{16}$$

It follows that the liquid yield of the system (utilizing Equation (15)) is (Barron 1985)

$$y = \frac{\dot{m}_f}{m} = \frac{h_1 - h_2}{h_1 - h_f} + x \frac{h_3 - h_e}{h_1 - h_f} \ . \tag{17}$$

The work requirement per unit mass compressed for the Claude method is equivalent to the Linde-Hampson when the expander is not used to aid compression (Barron 1985). Otherwise, the expander work expression is given by (Barron 1985)

$$\dot{W}_e = \dot{m}_e \left(h_3 - h_e\right) . \tag{18}$$

Therefore, the comprehensive work requirement per unit mass compressed for the specified Claude method is given by Equation (19). The last term shows the reduced work requirement coming from the expander (Barron 1985).

$$-\frac{\dot{W}}{\dot{m}} = \left(T_1\left(s_1 - s_2\right) - \left(h_1 - h_2\right)\right) - x\left(h_3 - h_e\right) \tag{19}$$

As previously, the T-s diagram in Appendix A provided all entropy and enthalpy values at the assumed temperatures and pressures.

From Equation (17) the liquid yield is then

$$y = \frac{h_1 - h_2}{h_1 - h_f} + x\frac{h_3 - h_e}{h_1 - h_f} = 0.262, \tag{20}$$

and the overall work requirement for per unit mass compressed for the Claude system from Equation (19) is

$$-\frac{\dot{W}}{\dot{m}} = \left(T_1\left(s_1 - s_2\right) - \left(h_1 - h_2\right)\right) - x\left(h_3 - h_e\right) = 815\frac{J}{g}. \tag{21}$$

It follows that the performance FOM of the Claude method of gas liquefaction (from Equation 2) is

$$FOM = \frac{\dot{W}_i / \dot{m}}{\dot{W} / \dot{m}_f} = 0.907. \tag{22}$$

As of 2020, Highview Power Storage Ltd. has the only operating LAES plant for commercial use in the world and utilizes a variation of the Claude method for gas liquefaction (Cochrane 2020). As shown, with the simple addition of an expander, assuming ideal conditions, the performance FOM was drastically improved compared to the Linde-Hampson method.

As seen in Figure 3, the method specified has 23 connection points, six nodes, and four unique node functions. Using Equations 3 and 4, it gives a system density score of 3.83 and an overall SCS of 15.3.

C. HEYLANDT METHOD

In 1949, Davies Mansel noted in his book, *The Physical Principles of Gas Liquefaction and Low Temp Rectification*, that when the Claude system was set to a higher pressure of 20 MPa (200 atm) and a flow-rate ratio to the expander of 60 percent, that the ideal temperature at the inlet of the expander was near ambient. Therefore, by increasing the pressure to 20 MPa, the first heat exchanger becomes unnecessary (Davies 1949). This modified system, shown in Figure 4 is called the Heylandt system. Today, "most high-pressure air liquefaction plants operate with the Heylandt process" (Hamdy et al. 2019, 8).

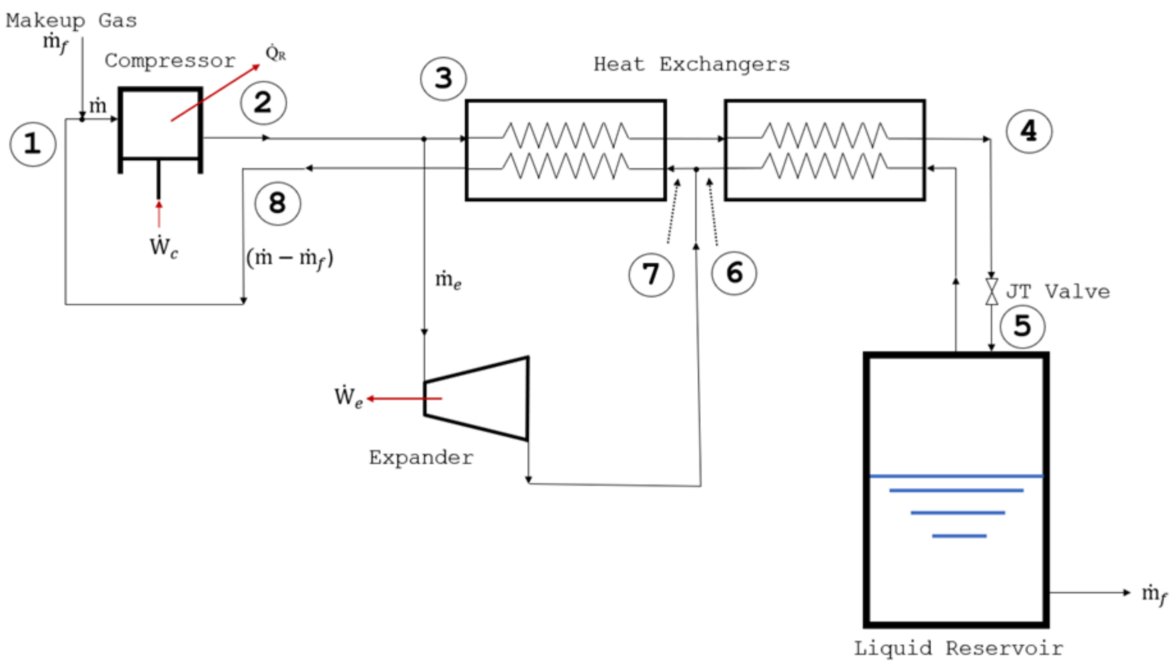

Figure 4. Heylandt Liquefaction System. Adapted from Barron (1985).

Due to the major similarities between the Claude method and Heylandt method, besides conditions of the working fluid at the inlet of the expander and a mass flowrate of 60 percent rather than 70, the calculations for performance are identical.

From Equation (17) the liquid yield is then

$$y = \frac{h_1 - h_2}{h_1 - h_f} + x\frac{h_3 - h_e}{h_1 - h_f} = 0.377, \tag{23}$$

and the overall work requirement for per unit mass compressed for the Heylandt system from Equation (19) is

$$-\frac{\dot{W}}{\dot{m}} = \left(T_1\left(s_1 - s_2\right) - \left(h_1 - h_2\right)\right) - x\left(h_3 - h_e\right) = 873\frac{J}{g}. \tag{24}$$

It follows that the performance FOM of the Heylandt method of gas liquefaction (from Equation 2) is

$$FOM = \frac{\dot{W}_i / \dot{m}}{\dot{W} / \dot{m}_f} = 0.846. \tag{25}$$

As seen in Figure 4, the method specified has 19 connection points, five nodes, and four unique node functions. Using Equations 3 and 4, it gives a system density score of 3.8 and an overall SCS of 15.2.

D. CASCADE METHOD

Today, the cascade method, or mixed refrigerant cascade (MRC), for cryogenic systems is used extensively for liquid natural gas (LNG) plants (Sanavandi, Mafi, and Ziabasharhagh 2019). However, the cascade method was the first method to be used to liquify air (Barron 1985). In 1933, W. H. Keesom proposed the cascade method shown in Figure 5 for gas liquefaction. A relatively low-pressure system, it uses ammonia to liquefy ethylene at 1925 kPa (19 atm), which in turn liquifies methane at 2530 kPa (25 atm), and lastly the methane is then used to liquefy nitrogen at 1885 kPa (18.6 atm) (Barron 1985). Similar to Keesom, a 1954 journal publication from Los Alamos laboratory by William Ball, suggested a similar cascade system as an extension of a precooling system that used only two Freon compounds (Ball 1954).

As Barron (1985) states in *Cryogenic Systems* "from a thermodynamic point of view, the cascade system is very desirable for liquefaction because it approaches the ideal reversible system more than [the Linde-Hampson cycle]" (Barron 1985, 84). However, unlike the previous methods, it is beyond this author's ability to generate a general equation for liquid yield. Therefore, this thesis only utilizes the observed results from Ball's experiments in 1954.

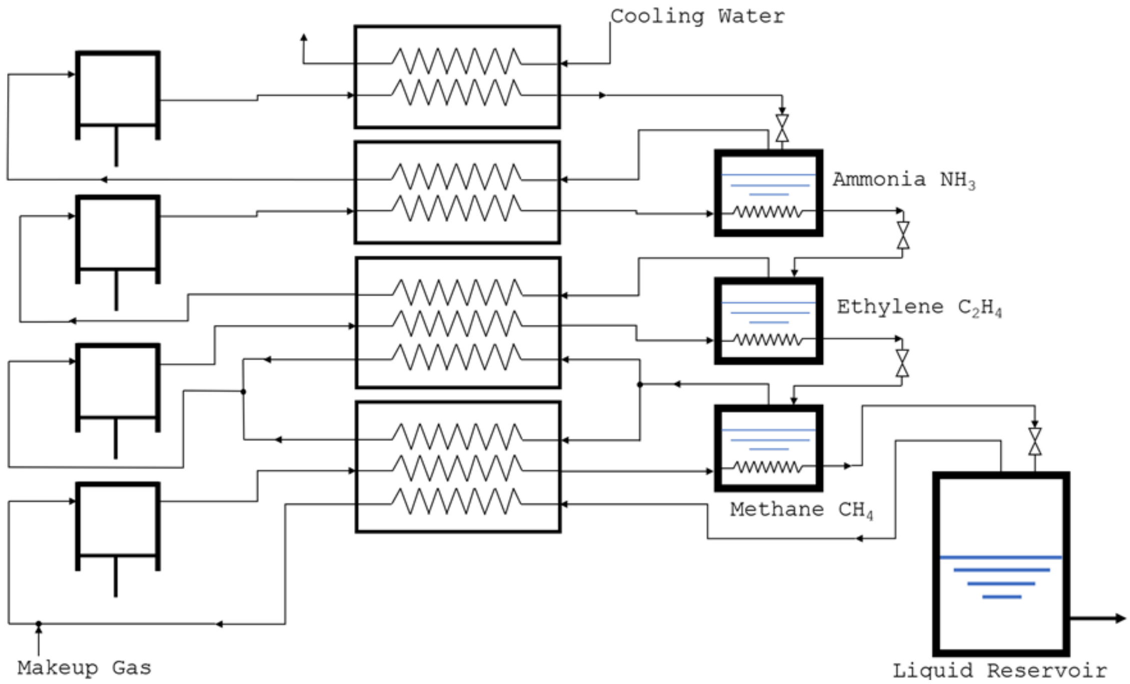

Figure 5. Cascade Liquefaction System. Adapted from Keesom (1933).

As seen in Figure 5, the method specified has 50 connection points, 12 nodes, and four unique node functions. Using Equations 3 and 4, it gives a system density score of 4.167 and an overall SCS of 16.7.

IV. RESULTS

Table 4 displays all the results of the theoretically derived FOM calculations alongside the experimentally observed PFOM values. Note that the observed work per unit mass liquified is roughly four times the calculated work for Claude and Heylandt methods and is roughly 1.75 times larger for the Linde-Hampson method. This useful comparison is a reminder of the importance of efficient heat exchangers and complete insulation from leaks or inlets from the ambient environment.

Table 4. Ideal, Theoretical, And Observed Performance Scores for Air Liquefaction Methods. Adapted from (Barron 1985).

Gas Liquefaction Method	Liquid Yield $\frac{\dot{m}_f}{m}$	Work per unit mass liquified (J/g) $-\frac{\dot{W}}{\dot{m}_f}$	Performance Figure of Merit $\frac{\dot{W}_i/\dot{m}}{\dot{W}/\dot{m}_f}$
Ideal Reversible System	1.000	738.9	1.000
Linde-Hampson	0.079	5,800.6	0.127
Claude	0.262	815	0.907
Heylandt	0.377	873	0.846
Linde-Hampson observed (Ruhemann 1949)	…	10,327	0.070
Claude observed (Ruhemann 1949)	…	3,582	0.201
Heylandt observed (Ruhemann 1949)	…	3,326	0.216
Cascade observed [Ball 1954)	…	3,256	0.221

Table 5 displays the calculation for a design solution given the four alternatives in which the stakeholder assigned equal weights to each MOP. The results show that the Heylandt method is the best selection for air-liquefaction method with a weighted final score of 0.9, with Cascade and Claude methods very close behind at 0.88 and 0.86. The Linde-Hampson was by far the worst performer with a final weighted score of 0.67.

Table 5. Design Solution for Equally Weighted Mop

	MOP	Performance FOM	System Complexity Score	Total
	Weight	0.5	0.5	1
Linde-Hampson	Raw	0.07	11	
	Scaled	0.348	1	
	Wtd	0.17	0.5	0.67
Claude	Raw	0.201	15.3	
	Scaled	1.000	0.719	
	Wtd	0.50	0.36	0.86
Heylandt	Raw	0.216	15.2	
	Scaled	1.075	0.724	
	Wtd	0.54	0.36	0.90
Cascade	Raw	0.221	16.7	
	Scaled	1.100	0.659	
	Wtd	0.55	0.33	0.88

Figure 6 and Figure 7 are the full design solutions for 11 differently weighted MOP variations. Figure 6 utilizes the theoretically derived values, and Figure 7 utilizes the observed values from Ruhemann’s and Ball’s experiments. Each cell applies the same method shown in Table 5, outputting the highest rated method for that set of inputs: Linde-Hampson (LH), Claude (CL), Heylandt (HT), and cascade (CA).

Performance FOM Weight (columns) / System Complexity Score Weight (rows)

	0	0.1	0.2	0.3	0.4	0.5	0.6	0.7	0.8	0.9	1
1	LH	LH	LH	LH	CL	CL	CL	CL	CL	CL	CL
0.9	LH	LH	LH	CL	CL	CL	CL	CL	CL	CL	CL
0.8	LH	LH	LH	CL	CL	CL	CL	CL	CL	CL	CL
0.7	LH	LH	LH	CL	CL	CL	CL	CL	CL	CL	CL
0.6	LH	LH	CL	CL	CL	CL	CL	CL	CL	CL	CL
0.5	LH	LH	CL	CL	CL	CL	CL	CL	CL	CL	CL
0.4	LH	LH	CL	CL	CL	CL	CL	CL	CL	CL	CL
0.3	LH	CL	CL	CL	CL	CL	CL	CL	CL	CL	CL
0.2	LH	CL	CL	CL	CL	CL	CL	CL	CL	CL	CL
0.1	LH	CL	CL	CL	CL	CL	CL	CL	CL	CL	CL
0	LH	CL	CL	CL	CL	CL	CL	CL	CL	CL	CL

Figure 6. Design Solution Matrix Given Theoretical Values

Performance FOM Weight (columns) / System Complexity Score Weight (rows)

	0	0.1	0.2	0.3	0.4	0.5	0.6	0.7	0.8	0.9	1
1	LH	LH	LH	LH	HT	HT	HT	HT	HT	HT	HT
0.9	LH	LH	LH	LH	HT	HT	HT	HT	HT	HT	HT
0.8	LH	LH	LH	LH	HT	HT	HT	HT	HT	HT	HT
0.7	LH	LH	LH	HT	HT	HT	HT	HT	HT	HT	HT
0.6	LH	LH	LH	HT	HT	HT	HT	HT	HT	HT	HT
0.5	LH	LH	HT	HT	HT	HT	HT	HT	HT	HT	HT
0.4	LH	LH	HT	HT	HT	HT	HT	HT	HT	HT	HT
0.3	LH	LH	HT	HT	HT	HT	HT	HT	CA	CA	CA
0.2	LH	HT	HT	HT	HT	HT	CA	CA	CA	CA	CA
0.1	LH	HT	HT	CA	CA	CA	CA	CA	CA	CA	CA
0	LH	CA	CA	CA	CA	CA	CA	CA	CA	CA	CA

Figure 7. Design Solution Matrix Given Observed Values

The Claude and Heylandt methods for air liquefaction show both the highest values for liquid yield and the highest levels of exergetic efficiency. The Linde-Hampson is by far the least effective alternative for air liquefaction, as seen in Table 4, but its simplicity is unmatched when compared to the alternatives. The cascade method, although not under comparison for theoretical performance, does retain the highest observed PFOM but requires serious planning considerations due it its high level of system complexity. The full design solutions provided in Figure 6 and Figure 7 are equally valuable and based on preference, however, theoretical calculations remove questions of ambient conditions, heat exchanger effectiveness, and other questions of possible design inefficiencies.

V. CONCLUSION

This paper presented the results of an analysis of alternatives that was designed around providing stakeholders with the necessary information to assist in selecting the appropriate liquefaction method for their set of given requirements. The implementation of new metrics for comparison, in system density and system complexity, are part of the vital process of providing new and useful tools for the emerging field of LAES and all cryogenic energy storage. Furthermore, the easy-to-use design solution matrices provide the simplification of LAES gas-liquefaction methods that is necessary for implementation and provide a template for further comparisons in future work that use other vital MOP.

A potentially fruitful avenue of future work lies in analyzing the individual scalability of these methods based on power requirements and size limitations. This can be done in analyzing varying methods giving set method designs, or by analyzing alternative nodes (e.g., axial versus centrifugal compressor) within a single liquefaction method for different power and size requirements. Although the provided design matrices are limited to two MOP, the method of additive weighting and scaling is not.

THIS PAGE INTENTIONALLY LEFT BLANK

APPENDIX

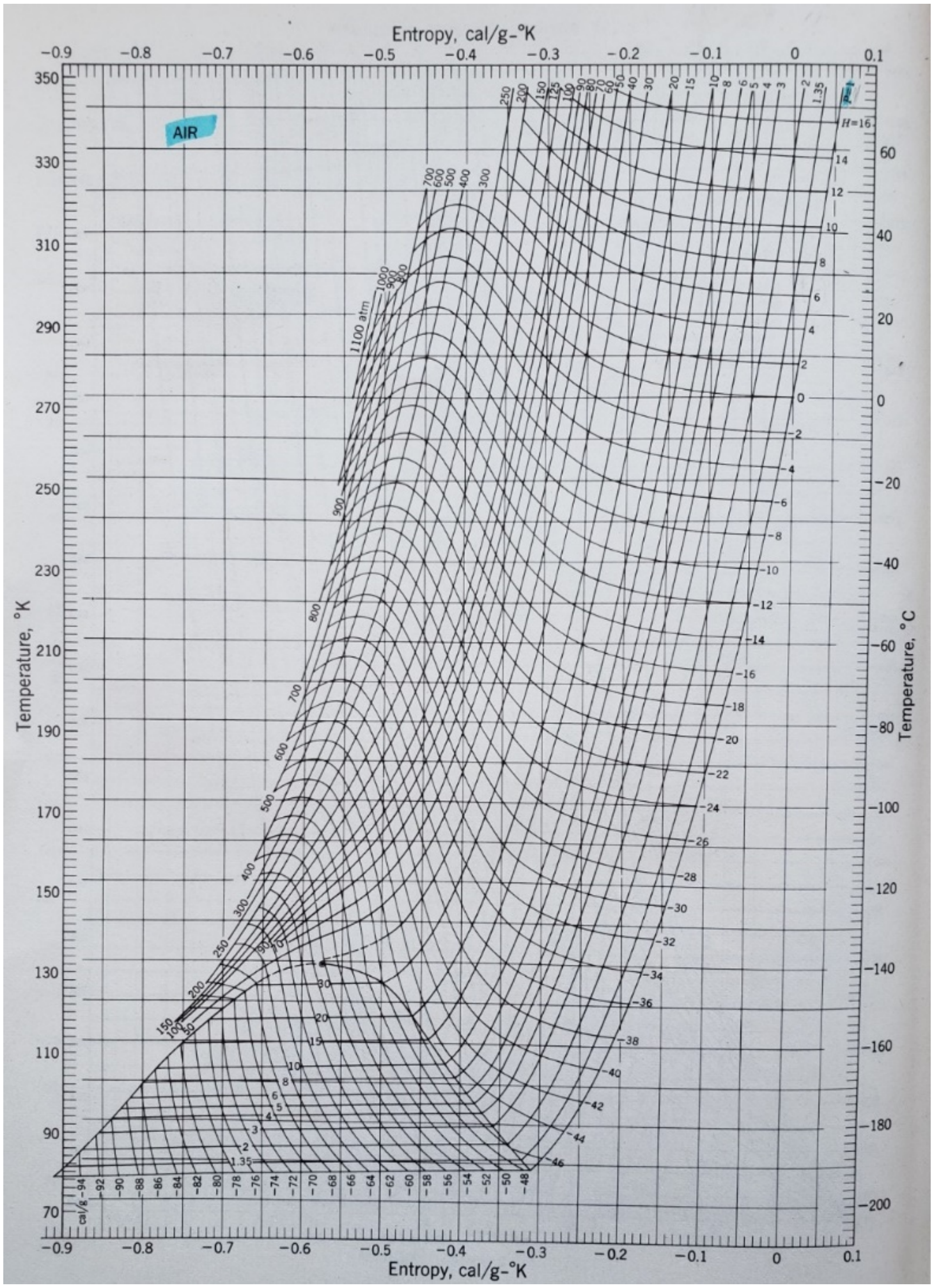

Figure 8. T-s Diagram for Air. Source: (Barron 1985).

THIS PAGE INTENTIONALLY LEFT BLANK

LIST OF REFERENCES

Ball, William. 1954. "Freon Cascade Refrigerator for Liquid Air Plant Precooler." *Refrigerating Engineering* 62: 54–46.

Barron, Randall F. 1985. *Cryogenic Systems*. 2^{nd} edition. Oxford University Press.

California Energy Commission. 2018. "Tracking Progress – Energy Storage." California Energy Commission. https://www.energy.ca.gov/sites/default/files/2019-12/energy_storage_ada.pdf.

Cochrane, J. 2020. Process Engineering Manager at Highview Power Ltd. Personal Correspondence.

Davies, Mansel. 1949. *The Physical Principles of Gas Liquefaction and Low Temperature Rectification*. Longmans, Green.

Denchak, Melissa. 2018. "Paris Climate Agreement: Everything You Need to Know." NRDC. December 12, 2018. https://www.nrdc.org/stories/paris-climate-agreement-everything-you-need-know.

Energy Storage Association. 2020. "Thermal Energy Storage Technology." 2020. https://energystorage.org/why-energy-storage/technologies/thermal-energy-storage/.

Eurostat. 2020. "Electricity Production, Consumption and Market Overview - Statistics Explained." Eurostat. July 31, 2020. https://ec.europa.eu/eurostat/statistics-explained/index.php/Electricity_production,_consumption_and_market_overview#Electricity_generation.

Graessler, Iris, Julian Hentze, and Tobias Bruckmann. 2018. "V-Models for Interdisciplinary Systems Engineering." In *DS 92: Proceedings of the DESIGN 2018 15th International Design Conference*, 747–56. https://doi.org/10.21278/idc.2018.0333.

Hamdy, Sarah, Francisco Moser, Tatiana Morosuk, and George Tsatsaronis. 2019. "Exergy-Based and Economic Evaluation of Liquefaction Processes for Cryogenics Energy Storage." *Energies (Basel)* 12 (3): 493-. https://doi.org/10.3390/en12030493.

Highview Power. 2020. "Liquid Air Energy Storage: Clean, Cost-Efficient, Flexible and Reliable." Highview Power. 2020. https://highviewpower.com/wp-content/uploads/2020/09/Highview-Brochure-Final-2020-1.pdf.

Högberg, Tomas, and Martin Tholander. 2018. “Evaluation of Liquid Air as an Energy Storage Alternative.” http://urn.kb.se/resolve?urn=urn:nbn:se:kth:diva-230095.

Howe, Todd A. 2018. “Thermodynamic System Analysis of a Liquid Air Energy Storage System.” Master’s thesis, Naval Postgraduate School.

IEA. 2020. “Global Energy Review 2020: The Impacts of the Covid-19 Crisis on Global Energy Demand and CO2 Emissions.” IEA. April 2020. https://www.iea.org/Textbase/npsum/MTrenew2014sum.pdf.

Jaraite, Jurate, Amin Karimu, and Andrius Kazukauskas. 2017. “Policy-Induced Expansion of Solar and Wind Power Capacity: Economic Growth and Employment in EU Countries.” *The Energy Journal* 38 (01). https://doi.org/10.5547/01956574.38.5.jjar.

Mills, Janet T. 2019. “An Order to Strengthen Main’s Economy and Achieve Carbon Neutrality by 2045.” Office of the Governor, Maine. https://www.maine.gov/governor/mills/sites/maine.gov.governor.mills/files/inline-files/Executive%20Order%209-23-2019_0.pdf.

Nelmes, Stuart. 2015. “Increasing Space Mission Ground Infrastructure Resiliency through Sustainability.” Madrid, Spain, November.

New York Department of Environmental Conservation. 2019. “Reducing Greenhouse Gas Emissions: Limiting Future Impacts of Climate Change.” Department of Environmental Conservation, New York State. 2019. https://www.dec.ny.gov/energy/99223.html.

Office of the Governor of Hawaii. 2018. “Governor’s Office – News Release – Governor David Ige Signs Bills to Set Carbon-Neutral Goal and Combat Climate Change.” Governor of the State of Hawaii. June 4, 2018. https://governor.hawaii.gov/newsroom/latest-news/governors-office-news-release-governor-david-ige-signs-bills-to-set-carbon-neutral-goal-and-combat-climate-change/.

Office of the Governor of New Mexico. 2019. “Governor Signs Landmark Energy Legislation, Establishing New Mexico as a National Leader in Renewable Transition Efforts.” Office of the Governor - Michelle Lujan Grisham. March 22, 2019. https://www.governor.state.nm.us/2019/03/22/governor-signs-landmark-energy-legislation-establishing-new-mexico-as-a-national-leader-in-renewable-transition-efforts/.

Pickard, William F. 2014. “Smart Grids Versus the Achilles’ Heel of Renewable Energy: Can the Needed Storage Infrastructure Be Constructed Before the Fossil Fuel Runs Out?” *Proceedings of the IEEE* 102, 7: 1094–1105. https://doi.org/10.1109/JPROC.2014.2316359.

REN21. 2020. “Renewables 2020 Global Status Report.” Paris, France: REN21 Secretariat. https://www.ren21.net/wp-content/uploads/2019/05/gsr_2020_full_report_en.pdf.

Ruhemann, M. 1949. *The Separation of Gases*. Fair Lawn, NJ: Oxford University Press.

Sanavandi, Hamid, Mostafa Mafi, and Masoud Ziabasharhagh. 2019. “Normalized Sensitivity Analysis of LNG Processes - Case Studies: Cascade and Single Mixed Refrigerant Systems.” *Energy (Oxford)* 188: 116068-. https://doi.org/10.1016/j.energy.2019.116068.

Seth, Lloyd. n.d. “Measures of Complexity a Non-Exhaustive List.” Massachusetts Institute of Technology.

Sixian, Wang, X.D. Xue, X.L. Zhang, J. Guo, Yuedan Zhou, and Wang Junjie. 2015. “The Application of Cryogens in Liquid Fluid Energy Storage Systems.” *Physics Procedia* 67 (December): 728–32. https://doi.org/10.1016/j.phpro.2015.06.123.

State of New Jersey. 2019. “Draft 2019 New Jersey Energy Master Plan Policy Vision to 2050.” State of New Jersey. https://nj.gov/emp/pdf/Draft%202019%20EMP%20Final.pdf.

Warner, Mark H. 2019. “Using V-Diagrams in Engineering Projects.” The Project Management Blueprint. October 28, 2019. https://www.theprojectmanagementblueprint.com/blog/procurements-management/the-v-diagram.

Washington State Department of Commerce. 2019. “Clean Energy Transformation Act (CETA).” May 7, 2019. http://www.commerce.wa.gov/growing-the-economy/energy/ceta/.

Watanabe, Osamu. 1992. *Kolmogorov Complexity and Computational Complexity*. 1st ed. Monographs in Theoretical Computer Science. An EATCS Series. Berlin, Heidelberg: Springer Berlin Heidelberg. https://doi.org/10.1007/978-3-642-77735-6.

THIS PAGE INTENTIONALLY LEFT BLANK

INITIAL DISTRIBUTION LIST

1. Defense Technical Information Center
   Ft. Belvoir, Virginia

2. Dudley Knox Library
   Naval Postgraduate School
   Monterey, California